Role of dust in landscape brightness and color

David K. Lynch

Thule Scientific, P.O. Box 953, Topanga, California 90290, USA (thule@earthlink.net)

Scattering by microscopic particles renders virtually all dusty surfaces brighter than dust-free surfaces. Examples of surface brightening are demonstrated in the landscape and laboratory and explained theoretically using Mie theory calculations. The implications for landscape photography and remote sensing are discussed.   © 2014 Optical Society of America

OCIS codes: (080.0080) Geometric optics; (240.0240) Optics at surfaces; (280.0280) Remote sensing and sensors; (330.1690) Color; (350.4990) Particles.

http://dx.doi.org/10.1364/AO.54.000B41

1. Introduction

Draw your finger across any surface, and it will remove the dust, revealing the underlying surface that is darker (cleaner) than the dusty one (Fig. 1). By dust, we mean any solid particle less than 125 μm in diameter. Examples are very fine sand, silt or clay, windborne soil, pollen, spores, volcanic dust, meteoritic dust, pollution particles, smoke particles, residue from water drops that have evaporated, and fibers from various sources such as spider webs and plant seeds. Household dust is composed of human hair and skin cells, dust mites, pollen, textile, and paper fibers. Dust-producing regions such as deserts cover approximately one-third of the global land area [1], and dust can be carried around the world.

Surface brightening happens because small particles of most any composition scatter light efficiently at visible wavelengths. Absorption by tiny particles is very small because their opacity parameter [23] $2\pi ka/\lambda$ is much less than unity (k is the imaginary part of the complex refractive index, a is particle radius, and λ is the wavelength of light). The brightness of a dusty surface may depend on the observer's line of sight relative to the Sun because of structure in the bidirectional reflectance distribution function.

Even if the dust is thick enough to hide the underlying surface, an opaque dust layer is often relatively bright unless the particles are highly absorbing. Indeed, think of the most common powders in everyday life: flour, household dust, powdered sugar, baby powder, baking powder and soda, cement, fertilizers, etc. Most of them are white or light colored, few are dark or black.

There is vast literature on light scattering by small particles. Equally large is the literature on dust because of its importance in remote sensing, geology, astronomy, optics, and computer graphic scene generation. In most cases, however, attention has been focused on a thick dust layer, as in the case of lunar soil or planetary regoliths such as sand dunes and comet surfaces. Much less attention has been paid to an optically thin dust layer and its influence on the color and brightness of a surface; for example, bare rock or plant leaves. Scattering by a single particle on a smooth surface has been studied in depth [4–9], but the broader notion of how particles that cover only a small fraction of a surface influence the reflected radiance has not been explicitly addressed to our knowledge.

In this paper, we investigate the brightening of natural surfaces due to light scattering by a small amount of dust. The original impetus for this work came from geological investigations, but the results reported here are applicable to natural surfaces of any kind.

2. Observations

While preparing for field work on the Lavic Lake Fault in California's Mojave Desert in 2014, the
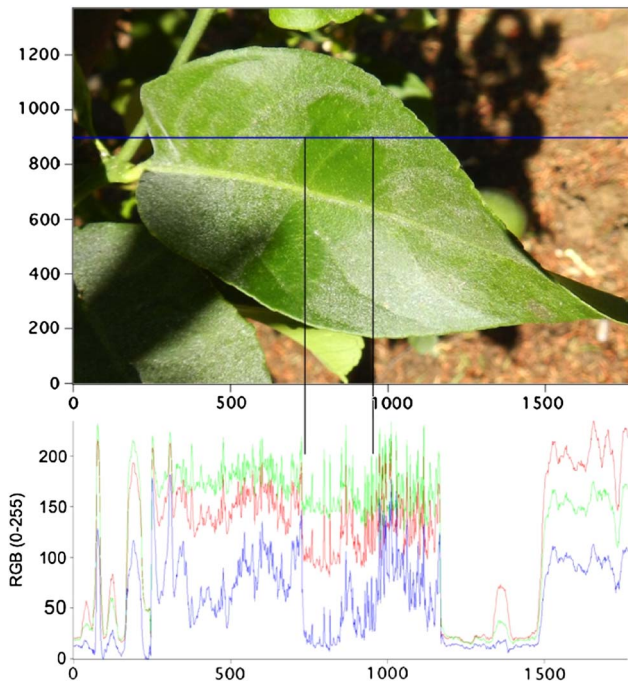
Fig. 1. Photograph of a leaf with a natural dust layer showing a section where the dust has been brushed off (upper). The clean leaf is clearly darker than its dusty surroundings. The lower plot shows an RGB scan across the image with the dust-free region marked by black vertical lines. Here each of the RGB brightnesses is depressed in the clean area.

author was surprised by how readily visible the fault trace was in overhead imagery (Fig. 2). Upon examining the fault in the field, the reason for its brightness became apparent: dust, or, to be more general, the presence and exposure of microscopically rough surfaces including dust. Examples include soil, minor landslides, scratched rocks, smashed rocks, and broken rock faces, the latter having fractal surfaces on microscopic scales [10,11] and thus are able to efficiently scatter light.

Fig. 2. Google Earth image of the Lavic Lake fault trace in the Mojave Desert in 2012, many years after the Hector Mine Earthquake (1999), which ruptured the surface. The fault trace is easily visible as a bright line through the landscape.

Fig. 3. Gravel surface along the fault. The upper photo shows the surface as the author found it in 2013. The lower picture shows the same scene but with one of the large cobbles overturned and displaced. The cobbles' dark upper surface is due to desert varnish. By overturning the rock, the dark face is hidden and bottom face is exposed. The bottom face is much lighter than even the rock itself due to the accumulation of pedogenic carbonates. Also, the lighter-colored underlying soil is revealed. As a result, the lower photo is brighter on average than the upper photo.

Much of the dust originated in the soil under the surface rocks. In desert environments, soil comes in large part from aeolian deposits with a large contribution from clay particles, which tend to be light colored. Obviously, wind can more easily loft and carry smaller particles than it can large ones. Thus desert soils have a high percentage of silt- and clay-size particles, typically <50 µm. At the fault plane itself, earthquake motion grinds rock into an extremely fine powder called gouge [12].

Several different though related effects involving microscopic surfaces have combined to brighten the fault trace. Minor landslides exposed lighter underlying soil and produced dust. Movement along the Lavic Lake fault during the Hector Mine earthquake did the same. Broken rocks displayed their lighter-colored interiors as well as exposed fractal-like fracture surfaces that efficiently scatter light. Overturned rocks exposed the light, underlying soil, and the now-hidden dark upper surfaces of the rock were hidden, thereby making the ground, on average, appear brighter (Fig. 3). In places where a shutter ridge blocked stream flow, alluvium pounded behind it until the stream cut through the ridge, leaving a small playa of light-colored soil, mostly clay.

3. Laboratory Results

While in the field, the author collected a number of rock samples along the fault; in this case, igneous extrusive cobbles and pebbles. Of particular interest were the darkest rocks such as basalt, a common

Fig. 4. Basalt pebble and a powdered fragment of it. The powder is brighter than the pebble itself.
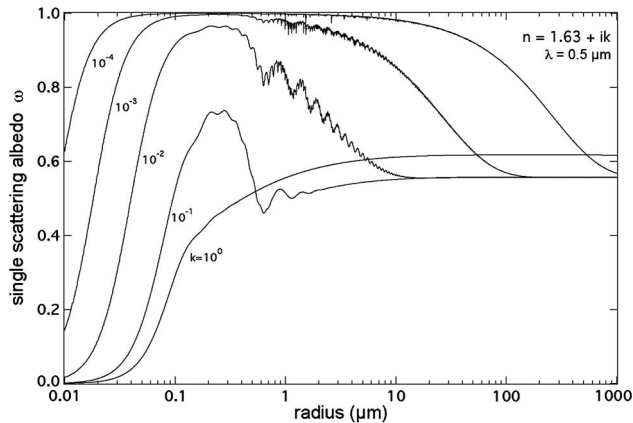

Fig. 5. Mie calculation of the single scattering albedo as a function of particle radius for a variety of values of the imaginary part of the index of refraction k. $k = 10^{-4}$ corresponds to a weakly absorbing material like quartz ($k = 10^{-7}$), while $k = 1$ corresponds to a strongly absorbing material like graphite. For $10^{-4} < k < 10^{-2}$, the single scattering albedo increases as the particle size decreases from 1000 μm. When the particle size enters the Rayleigh regime, the single scattering albedo decreases rapidly. Only the relatively rare, highly absorbing particles ($k > 10^{-2}$) do not show this behavior. Thus, small particles of most materials are brighter than large particles of the same material.

black rock high in Fe and Mg and low in Si. In the laboratory, basalt pebbles were sanded flat on one side, and then tiny pieces were ground into powder (Fig. 4). The roughened surfaces and powders were considerably brighter than the original rock, showing again that small particles of rock are brighter than large particles of it. This is hardly a surprise because geologists have been using the "streak test" to help identify rocks since antiquity. A rock drawn across the surface of an unglazed ceramic tile leaves a streak of finely powdered rock whose color can be indicative of the rock's composition. The revealing value of a streak can be illustrated in the following example: hand specimens of magnetite and biotite are both black, but their streaks are quite different; black and white, respectively.

Having briefly reviewed the well-known but seldom mentioned fact that powders of almost any material are usually brighter than the bulk samples from which the powder was derived, we now turn to the reasons for this.

4. Mie Calculations

Figure 5 shows Mie calculations using MiePlot [13] of single scattering albedo ω at wavelength 0.5 μm as a function of particle radius for $n = 1.63 + ik$ where k was varied by factors of 10 between 10^{-0} and 10^{-4}. These values were chosen to span the refractive indices of common dust compositions (Table 1). Many small particles such as pollen and rock dust are compositionally heterogeneous. Therefore, a single refractive index is difficult to measure and does not represent the whole particle. The Mie calculations refer to spherical particles, and dust particles are certainly not spherical. However, the physical interpretation is much the same, and the computation demonstrates the general situation for nonspherical particles.

Table 1. Complex Refractive Indices for Common Dust Compositions

Dust Composition	Approximate Wavelength (nm)	Real n	Imaginary k	Reference
Quartz	500	1.54(o) 1.55(e)	1E − 7	Various
Calcite	500	1.65(o) 1.49 (e)	—	Various
NaCl	500	1.54	—	Various
Illite	500	1.57	0.001	Various, especially [14]
Montmorillonite	500	1.5	5E − 05	Various, especially [14]
Kaolinite	500	1.56	0.0001	Various, especially [14]
Basalt	500	1.63	0.01	[15]
Limonite	500	2.16	0.13	[15]
Dolomite	500	1.62		Reported in [16]
Gypsum	500	1.52	3E − 06	[17]
Hematite	500	3.05	0.3	Reported in [16]
Urban aerosols	532	1.59	0.044	[18]
Polystyrene	500	1.59	5E − 04	[19]
Soot	500	1.5	0.47	Reported in [16]
Saharan dust	505	1.47 − 1.59	0.01 − 0.0013	[20]
Saharan dust	500	1.56 − 1.59	3E − 7–7E − 7	[16]
Atmospheric dust	500		2E − 3 − 0.01	Reported in [21]
			−means < 1E − 4	

For $k = 10^{-4}$ & 10^{-3}, the albedo increased to near unity as the particle size decreased from 1000 μm to about 0.5 μm. With further decrease in particle size, ω entered the Rayleigh regime and decreased. For $k = 10^{-2}$, the albedo increased, however, with small-scale variations to a maximum of about 0.98 before decreasing as the particle sizes entered the Rayleigh regime. Highly absorbing particles typical of hematite and soot ($k > 10^{-2}$) showed more complex behavior, and, for $k = 10^{-0}$, the particle's albedo decreased monotonically with decreasing particle size. Although relatively few rocks have had their complex refractive indices measured because of natural variations from sample to sample, most have $k < 10^{-2}$, and thus their powders and streaks are relatively bright.

5. Discussion

The amount of light reflected from a dusty surface will depend on the fractional surface coverage and albedo of the dust. The effect is most pronounced for dark surfaces. A bright surface such as limestone or chalk would show little if any brightening. Indeed, light surfaces could darken a bit if the dust tended to absorb light. In most cases, however, brightening will occur because rocks and plants are relatively dark, the albedos of most of the Earth's land surfaces being about 0.2 in the absence of snow [22]. The "whitening" of surfaces is very much like a fading color. It can be viewed as a color shift in the surface's International Commission on Illumination (CIE) chromaticity coordinates toward the achromatic point (Fig. 6). Note that highly absorbing ("black") powders will have similar trajectories in the CIE

color space, but instead of brightening the surface, they will darken it.

The presence of dust has not prevented the satellite and airborne communities from retrieving vast amounts of useful spectral data from their imagery. Thus, it seems that dust has been unknowingly accommodated in retrieval algorithms, at least until it becomes thick enough to confuse the retrieval system. The situation is identical to what occurs in any imaging system whose pixel size or resolution does not resolve the surface in sufficient detail to separate different components. The observed spectra are composites of spectra of all the different materials within a resolution element. The approach to "unmixing" the spectra is to add various candidate spectra together in various proportions in an effort to match the observed spectra.

Even macroscopically smooth surfaces are microscopically rough and, thus, can be thought of as having a "dust-like" coating. Microscopic upward (and downward) projections will scatter light differently than will the smooth bulk material. Light scattering is useful in determining surface rugosity [23].

Earthquakes are known to raise vast dust clouds, especially in desert regions [24]. The main reason is that falling rocks (i.e., landslides on every scale) collide with other rocks, and the impacts produce many small particles. Indeed, any violent event such as forest fires, explosions, strong desert winds, volcanic eruptions, or building collapses generate large amounts of dust, and loft it high into the atmosphere where it may be carried great distances before settling to the ground.

6. Summary and Conclusions

We have demonstrated the optical effects that lead to surface brightening by thin dust layers and explained them theoretically using Mie calculations. In general, the smaller the particle, the brighter and whiter it is. Surface brightening is the result of light scattered by dust particles that absorb very little incident light by virtue of being very small or having small imaginary parts of their refractive index ($k < 10^{-2}$), or both.
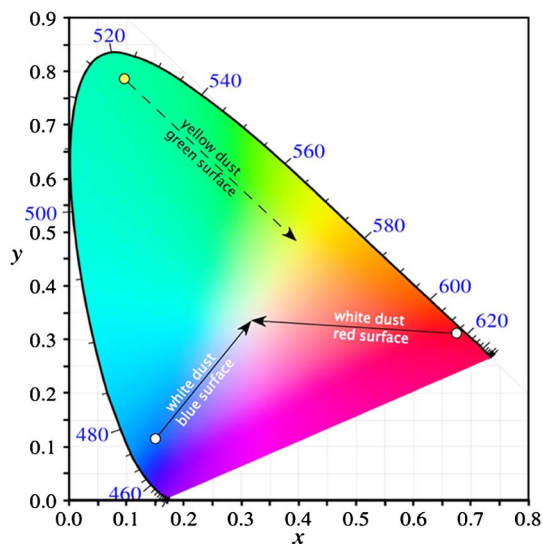
Fig. 6. Notion trajectories of surface colors as dust is deposited on them. The solid arrows show the paths of color of the surface, as it grows whiter with increasing amounts of dust. Starting with no dust (white open circles) at the coordinates of the surface's intrinsic color, the colors fade until reaching the achromatic point when dust covers 100% of the surface. We have assumed that the dust particles are white and opaque and that no multiple scattering takes place. If the dust has color (dashed arrow), the trajectory will be from the clean surface color to the dust's color.

References
1. T. D. Jickells, Z. S. An, K. K. Andersen, A. R. Baker, G. Bergametti, N. Brooks, J. J. Cao, P. W. Boyd, R. A. Duce, K. A. Hunter, H. Kawahata, N. Kubilay, J. Laroche, P. S. Liss, N. Mahowald, J. M. Prospero, A. J. Ridgwell, I. Tegen, and R. Torres, "Global iron connections between desert dust, ocean biogeochemistry, and climate," Science **308**, 67–71 (2005).
2. D. K. Lynch and S. Mazuk, "On the size parameter for thermally emitting particles," Appl. Opt. **38**, 5229–5231 (1999).
3. D. K. Lynch and S. Mazuk, "Size parameter for thermally emitting particles: erratum," Appl. Opt. **38**, 7467 (1999).
4. J. F. Blinn, "Light reflection functions for simulation of clouds and dusty surfaces," in *SIGGRAPH '82 Proceedings*

of the 9th Annual Conference on Computer Graphics and Interactive Techniques (ACM, 1982).

5. G. W. Videen, W. L. Wolfe, and W. S. Bickel, "Light scattering Mueller matrix for a surface contaminated by a single particle in the Rayleigh limit," Opt. Eng. **31**, 341–349 (1992).

6. E. Fucile, P. Denti, F. Borghese, R. Saija, and O. I. Sindoni, "Optical properties of a sphere in the vicinity of a plane surface," J. Opt. Soc. Am. A **14**, 1505–1514 (1997).

7. B. R. Johnson, "Light diffraction by a particle on an optically smooth surface," Appl. Opt. **36**, 240–246 (1997).

8. G. Videen, "Light scattering from a sphere near a plane interface," in *Light Scattering from Microstructures, Lecture Notes in Physics* (Springer, 2000), Vol. **534**, pp. 81–96.

9. J. Gu, R. Ramamoorthi, P. Belhumeur, and S. Nayar, "Dirty glass: rendering contamination on transparent surfaces," in *Proceedings of Eurographics Symposium on Rendering (EGSR'07)*, J. Kautz and S. Pattanaik, eds. (Eurographics Association, 2007).

10. A. Carpenteri and B. Chiaia, "Multifractal nature of concrete fracture surfaces and size effects on nominal fracture energy," Mater. Struct. **28**, 435–443 (1995).

11. T. Ficker, "Fractality of fracture surfaces," Acta Polytechnica **50**, 26–31 (2010).

12. F. T. Wu, "Mineralogy and physical nature of clay gouge," Pure Appl. Geophys. **116**, 655–689 (1978).

13. P. Laven, 2014, http://www.philiplaven.com/mieplot.htm.

14. I. N. Sokolik and O. B. Toon, "Incorporation of mineralogical composition into models of the radiative properties of mineral aerosol from UV to IR wavelengths," J. Geophys. Res. **104**, 9423–9444 (1999).

15. W. G. Egan and J. F. Becker, "Determination of the complex index of refraction of rocks and minerals," Appl. Opt. **8**, 720–721 (1969).

16. K. Kandler, N. Benker, U. Bundke, E. Cuevas, M. Ebert, P. Knippertz, S. Rodriguez, L. Schutz, and S. Weinbruch, "Chemical composition and complex refractive index of Saharan Mineral Dust at Izaña, Tenerife (Spain) derived by electron microscopy," Atmos. Environ. **41** 8058–8074 (2007).

17. T. L. Roush, F. Esposito, G. R. Rossman, and L. Colangeli, "Estimated optical constants of gypsum in the regions of weak absorptions: Application of scattering theories and comparisons to independent measurements," J. Geophys. Res. **112**, E10004 (2007).

18. J.-C. Raut and P. Chazette, "Retrieval of aerosol complex refractive index from a synergy between lidar, sunphotometer and in situ measurements during LISAIR experiment," Atmos. Chem. Phys. **7**, 2797–2815 (2007).

19. X. Ma, J. Q. Lu, R. S. Brock, K. M. Jacobs, P. Yang, and X.-H. Hu, "Determination of complex refractive index of polystyrene microspheres from 370 to 1610 nm," Phys. Med. Biol. **48**, 4165–4172 (2003).

20. R. Wagner, T. Ajtai, K. Kandler, K. Lieke, C. Linke, T. Müller, M. Schnaiter, and M. Vragel, "Complex refractive indices of Saharan dust samples at visible and near UV wavelengths: a laboratory study," Atmos. Chem. Phys. **12**, 2491–2512 (2012).

21. I. N. Sokolik, A. Andronova, and T. C. Johnson, "Complex refractive index of atmospheric dust aerosols," Atmos. Environ. **27**, 2495–2502 (1993).

22. D. A. Rutan, T. P. Charlock, F. G. Rose, S. Kato, S. Zentz, and L. Coleman, "Global surface albedo from CERES/TERRA surface and atmospheric radiation budget (SARB) data product," in *Proceedings of 12th Conference on Atmospheric Radiation*, Madison, Wisconsin, 10–14 July, 2006.

23. A. A. Maradudin, ed., in *Light Scattering and Nanoscale Surface Roughness* (Springer, 2007), p. 496.

24. http://www.youtube.com/watch?v=gPKVIW6lymM